A New Variant Selection Criterion for Twin Variants in Titanium alloys (Part 2).

By Christophe Schuman, Lei Bao, Jean Sébastien Lecomte, Yudong Zhang, Jean Marc Raulot, Marie Jeanne Philippe, Claude Esling

Laboratoire d'Étude des Microstructures et de Mécanique des Matériaux, LEM3, CNRS 7239, Université Paul Verlaine – Metz, Ile du Saulcy, 57045 Metz, France

A new selection criterion to explain the activation of the twinning variant is proposed. This criterion is based on the calculation of the deformation energy to create a primary twin. The calculation takes into account the effect of the grain size using a Hall-Petch type relation. This criterion allows to obtain a very good prediction for the twin family selection and twin variant selection. The calculations are compared with the experimental results obtained on T40 (ASTM grade 2) deformed by Channel Die compression.

Introduction

Deformation twinning is one of the main deformation modes in crystalline solids particularly in low symmetry or multiple lattice structures [1-8]. Though extensive studies have addressed on the crystallography [9-11], morphology [12] and mechanical behavior [2, 13] of deformation twins, and numerous models for twinning over the last few decades [14, 15], some fundamental issues remain unclear. The nucleation and growth mechanism of twin lamellae, the interaction of twinning with crystal defects, and the interfacial accommodation between the matrix and the twins [16, 17] are still poorly understood.

In the case of titanium alloys, many authors have attempted to determine the presence of the different types of twins as a function of the deformation temperature or grain size [18, 19, 24] as well as to extract useful information for modeling [1, 20].

Although the twin type and the twin volume fraction can be easily determined [21], the type of variants present as well as the sequence in which they appear in one grain are not well revealed.

Recently, we have developed the "interrupted in situ SEM/EBSD orientation examination method" to follow the microstructure and crystallographic orientation evolution during the

mechanical deformation process. This method allows us to obtain the time resolved information of the appearance of the twin variants, their growth, the interaction between them and the interaction with the initial grain boundaries [22]. However, the variant selection rules and the physical mechanisms behind still remain uncovered.

For magnesium and magnesium alloys that are also hexagonal materials but with different c/a ratio from that of titanium [17], Martin [26] and Jonas [27] have proposed variant selection rules (Schmid Factor (SF), common volume) for the secondary twinning during deformation. Their criteria worked well for the deformed magnesium where the twins are thin. However, for titanium, it seems that the selection of the variants follows a different rule and should be clarified.

In the present work, we experimentally investigated the deformation process of commercially pure titanium with interrupted in situ SEM/EBSD orientation measurements. Based on the experimental examination, we tried to work out the twin variant selection rule. This rule is not established by a more statistical examination to have statistical representation but to reveal the physical and mechanical criteria (energy) of variant selection that would be useful for the modeling of the mechanical behavior of the alloys.

Material and Sample preparation

The material was hot-rolled and then annealed commercially pure titanium sheet of 1.5 mm thick with the composition given in table 1.

Table 1 Chemical composition of commercially pure titanium T40

Element	H	C	N	O	Fe	Ti
Composition (ppm(wt.))	3	52	41	1062	237	Balance

A grain growth annealing was performed at 750°C for 2 hours to produce a fully recrystallized microstructure. After annealing, the samples were mechanically ground up to 4000 #-grit SiC paper and then electrolytically polished at 5°C and 17V for 30 seconds in a solution of 10 ml perchloric acid in 90 ml methanol.

The samples were channel die compressed in two passes, first with 8 % and then 16% reduction. To follow the rotation of the individual grains during the deformation, a 500×300 μm^2 area was carefully polished and marked out with four micro-indentations. The orientation of all the grains in this polished area (about 800 grains) was measured by SEM/EBSD before and after each deformation step. Fig. 1 is the sketch of the channel die compression. Before each compression, the two sample plates as shown in Fig. 1 were firmly stuck together to avoid sliding during the compression in order to maintain a good surface quality [22].

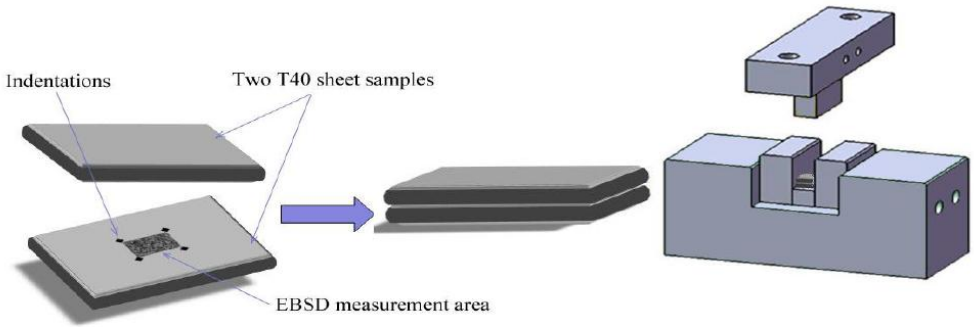

Figure 1: Schematic description of the channel-die set-up used.

Crystallography and identification

The grain size of the sample ranges from 150 to 250µm. It is well known that such large grains favour the formation of twins during deformation. We have examined more than 80 grains in this individual follow-up and identified all the twin types, their variants and their order of appearance. We found only compressive twin ($(11\bar{2}2)$ or C Type) and tension twin ($(10\bar{1}2)$ or T1 type) (see table 2), and we did not find T2 or $(11\bar{2}1)$ tension twin. The

activation of these twins depends only on the initial orientation of the grain and the local stress tensor which is a function of the applied forces. Furthermore with the increase of the deformation, secondary twins appear inside primary twins: T1 tension twins inside C compression twins or C compression twins inside T1 tension twins. Generally these second generation of twins are called secondary or double twin.

Table 2: list of slip and twin systems in Titanium

Slip/Twin	$\vec{b}$	Slip system	Notation
Basal	<a>	$\{0002\}[11\bar{2}0]$	B<a>
Prismatic	<a>	$\{1\bar{1}00\}[11\bar{2}0]$	P<a>
Pyramidal π_1	<a>	$\{1\bar{1}01\}[11\bar{2}0]$	π_1<a>
Pyramidal π_1	<c+a>	$\{1\bar{1}01\}[11\bar{2}\bar{3}]$	π_1<c+a>
Pyramidal π_2	<c+a>	$\{1\bar{1}22\}[11\bar{2}\bar{3}]$	π_2<c+a>
Tension Twin	--	$\{10\bar{1}2\}[\bar{1}011]$	T1
Tension Twin	--	$\{11\bar{2}1\}[\bar{1}\,\bar{1}26]$	T2
Compression Twin	--	$\{11\bar{2}2\}[\bar{1}\,\bar{1}23]$	C

To identify the type of twin system and the active variants (Table 3) that accommodate the plastic deformation, trace analysis is used (Fig 2).

Table 3: list of variants for two type of twins twin

Compression C		Tension T1	
CV1	$(11\bar{2}2)\langle 11\bar{2}\bar{3}\rangle$	**T1V1**	$(10\bar{1}2)\langle\bar{1}011\rangle$
CV2	$(\bar{2}112)\langle\bar{2}11\bar{3}\rangle$	**T1V2**	$(\bar{1}102)\langle 1\bar{1}01\rangle$
CV3	$(\bar{1}\bar{1}2\bar{2})\langle 11\bar{2}\bar{3}\rangle$	**T1V3**	$(\bar{1}012)\langle 10\bar{1}1\rangle$
CV4	$(1\bar{2}12)\langle 1\bar{2}1\bar{3}\rangle$	**T1V4**	$(0\bar{1}12)\langle 01\bar{1}1\rangle$
CV5	$(2\bar{1}\bar{1}2)\langle 2\bar{1}\bar{1}\bar{3}\rangle$	**T1V5**	$(1\bar{1}02)\langle\bar{1}101\rangle$
CV6	$(\bar{1}2\bar{1}2)\langle\bar{1}2\bar{1}\bar{3}\rangle$	**T1V6**	$(01\bar{1}2)\langle 0\bar{1}11\rangle$

Twinning is treated as a slip system to calculate the Schmid Factor (SF). Also the trace angles of all possible twin planes on the grain surface are calculated with respect to the sample coordinate system. Then the trace angles of the observed twin planes are measured in the same coordinate system and compared with the calculated ones to identify the corresponding active twin system and twin variant. The schematic of the position of a slip line (or twin line) on the sample surface is shown in Fig 2.

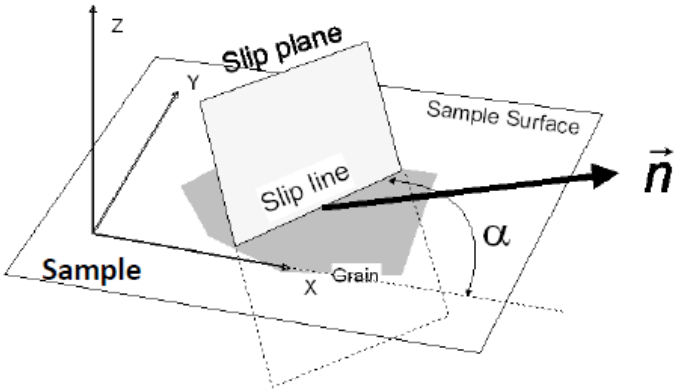

Figure 2 : Slip (twin) line trace on the sample surface.

Figure 3 follows step by step the onset of primary and secondary twin. The results show that the twin variants that appear in the grain to accommodate the deformation are seldom those with the highest SF. In fact, only less than 50% of the variants with the highest SF are selected. Often in the equiaxed grains, several twin variants can appear, whereas in those with elongated shape, only one variant appears, but it appears repeatedly, as shown in Fig. 3 b. This indicates that the shape of the initial grain also influences the selection of the variants.

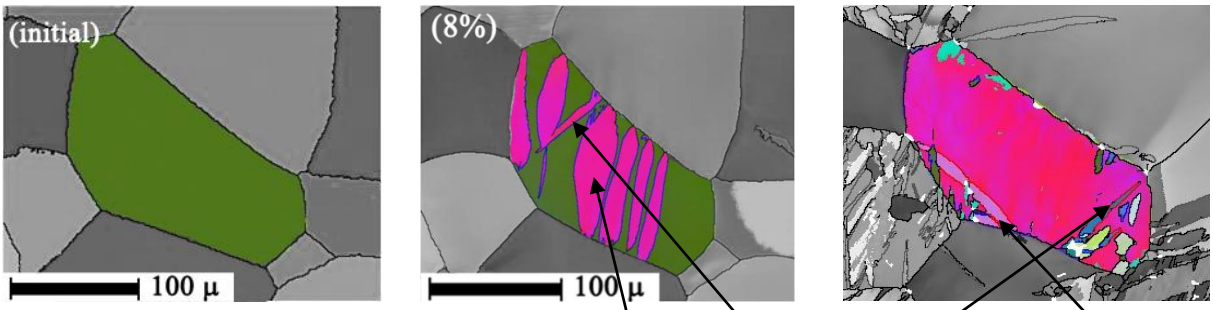

a) Orientation of the initial matrix :(104.4, 27.7, 50.8)

b) Tension twin : T1V6 and T1V4 (2 variants with the same orientation)

c) Compression twin: CV1, CV6
Orientation of the new twin matrix :(162.4, 20.9, 38.9)

Figure 3: a) initial grain; b) with one variant after 8 % deformation ; c) same grain after 16% deformation, with multiple variants (the initial matrix disappear totally)

Deformation Energy

The decrease of the internal energy of the material must be sufficient to deliver the energy to create (to propagate) the twin. To calculate this plastic deformation energy in a grain we have made some assumptions:

-The material is an ideal (i.e., no strain hardening) rigid- plastic body,

-The material obeys the Von Mises (VM) yield criterion (here, each type of twin has its own yield stress (note σ_y) expressed in the sample frame),

- The stress applied to a grain is the same as that applied to the sample. (Sachs assumption),

- Due to the geometry of channel die set-up, there is no width of the sheet. This corresponds to material flow in plane strain in the principal axes 1 and 3. The components of the stress tensor are supposed to remain constant in the thickness. The calculations are made at the neutral fiber.

Under these assumptions the strain and stress tensor have the following form :

$$\bar{\bar{\epsilon}} = \begin{pmatrix} \epsilon_{11} & 0 & 0 \\ 0 & 0 & 0 \\ 0 & 0 & \epsilon_{33} \end{pmatrix} \quad (1)$$

$$\bar{\bar{\sigma}} = \begin{pmatrix} \sigma_{11} & 0 & 0 \\ 0 & \sigma_{22} & 0 \\ 0 & 0 & \sigma_{33} \end{pmatrix} \quad (2)$$

Considering the state of plane strain on the edge of the plastic flow just at the limit of the elastic range, the following relation holds:

$\sigma_{22} = \frac{1}{2}(\sigma_{11} + \sigma_{33})$ (3)

In this case the VM criterion is:

$\sigma_{11} - \sigma_{33} = \frac{2}{\sqrt{3}}\,\sigma_y$ (4)

Also, since work material volume is constant in plastic deformation : $\epsilon_{11} = -\epsilon_{33}$ (5)

As the material is a rigid plastic body for twinning, we can easily calculate the plastic strain energy (per unit volume) with the relations above:

$$W = \epsilon_{11}\sigma_{11} + \epsilon_{33}\sigma_{33} \quad (6)$$

If we introduce Eq. (5) into Eq. (6), we have:

$$W = -\epsilon_{33}\sigma_{11} + \epsilon_{33}\sigma_{33} = -\epsilon_{33}(\sigma_{11} - \sigma_{33}) \quad (7)$$

Substituting Eq. (4) into Eq. (7) we obtain:

$$W = -\frac{2}{\sqrt{3}}\,\sigma_y\epsilon_{33}. \quad (8)$$

In the latter equation, ϵ_{33} is the macroscopic strain. Reed-Hill[29] and Tenckhoff[30] have shown that the macroscopic strain is related to the strain produced by the twins multiplied by their volume (V).

Hence:

(6) is the macroscopical $\epsilon_{33} = V\epsilon'_{33}$ (9)

with ϵ'_{33} being the twinning deformation expressed in the sample coordinate frame

Then, the plastic deformation becomes:

$$W = -\frac{2}{\sqrt{3}}\,V\sigma_y\epsilon'_{33} = \frac{2}{\sqrt{3}}\,V\,W_{twin} \quad (10)$$

with

$$W_{twin} = \tau\gamma|_{twin\ frame} = -\sigma_y\varepsilon'_{33}\big|_{sample\ frame} \quad (11)$$

where σ_y is the critical resolved shear stress required (=shear stress τ in twin frame expressed in the sample frame) to activate the twinning system and ε'_{ij} is the corresponding twinning

deformation. The twinning system will be active when the resolved shear stress reaches the corresponding critical value σ_y.

The displacement gradient tensor was first expressed in an orthonormal reference frame defined by the related twinning elements [28]. The unit vector normal to the twinning plane, the unit vector normal to the shear plane and the unit vector in the twinning direction define this reference frame. In this frame the displacement gradient tensor has a particularly simple form:

$$e_{ij} = \begin{pmatrix} 0 & 0 & s \\ 0 & 0 & 0 \\ 0 & 0 & 0 \end{pmatrix} \quad (12)$$

With $s = \frac{|\gamma^2-3|}{\gamma\sqrt{3}}$ for the (10-12) twin and $s = \frac{2(\gamma^2-2)}{3\gamma}$ for the (11-22) twin where $\gamma = {}^{c}/_{a}$ ratio of titanium[9] , the displacement gradient tensor for the two types of twins can be obtained as:

Compression (11-22) Tension (10-12)

$$\begin{pmatrix} 0 & 0 & 0.218 \\ 0 & 0 & 0 \\ 0 & 0 & 0 \end{pmatrix} \qquad \begin{pmatrix} 0 & 0 & 0.175 \\ 0 & 0 & 0 \\ 0 & 0 & 0 \end{pmatrix} \quad (13)$$

Through coordinate transformation, this displacement gradient tensor can be expressed in the crystal coordinate system (here we choose the orthonormal reference system set to the hexagonal crystal basis and the setting follows the Channel 5 convention, i.e. $e_2//a_2$ and $e_3//c$). With the Euler angles measured by SEM/EBSD that represent a set of rotations from the sample coordinate system to the orthonormal crystal basis, this tensor can be further transformed into the macroscopic sample coordinate system. If G is the coordinate transformation matrix from the macroscopic sample coordinate system to the orthonormal

twin reference system, the displacement gradient tensor with respect to the sample coordinate system can be expressed as:

$$(e_{ij}^{sample\ frame}) = G(e_{ij}^{crystal\ frame})G^{-1} \quad (14)$$

Thus the deformation tensor in the macroscopic sample coordinate system can be obtained as the symmetrized displacement gradient:

$$\varepsilon'_{ij} = \frac{1}{2}(e_{ij} + e_{ji}) \quad (15)$$

With Eq. (15), the strain term can thus be calculated.

Results

The strain term ε'_{33} in Eq. (11) has been calculated for all the examined grains with the two cases of primary twinning, with tension twin (T1) and with compression twin (C). The results are shown in Table 4. The cases for secondary twinning are shown in Table 5. It should be noted that in a primary tension twin, only secondary compression twin can form and vice versa. In the table, the orientation of the grain is given by the Euler angles (φ_1, ϕ, φ_2) with respect to the macroscopic sample coordinate system and is measured by EBSD/SEM.

With the experimental orientation, the SF and the ε'_{33} are calculated for all the twin variants (both tension and compression type). The experimentally observed active variant is highlighted in gray in all the tables. The maximum SF of the variants is in bold. It is seen that the activated variants are not those with the highest SF. We can also see that the values of ε'_{33} are sometimes negative and sometime positive. It depends on the grain orientation and on the type of twins.

Table 4: Calculation of SF and ε'_{33} for different orientations and twin families

	Orientation of grain: {92.4, 23.5, 53.4}		Orientation of grain:{111.5, 20.5, 34.5}		Orientation of grain:{93, 86.8, 9.6}		Orientation of grain:{54.5, 80.8, 7.6}	
C twin	SF	ε'_{33}	SF	ε'_{33}	SF	ε'_{33}	SF	ε'_{33}
CV1	**0,465**	-0,101	0,0729	-0,016	0,166	0,036	0,110	0,024
CV2	0,305	-0,067	0,3708	-0,081	0,045	0,010	0,026	0,006
CV3	0,152	-0,033	0,4200	-0,092	0,197	0,043	0,194	0,042
CV4	0,260	-0,057	**0,4201**	-0,092	**0,459**	0,100	**0,488**	0,106
CV5	0,431	-0,094	0,3073	-0,067	0,062	0,013	0,078	0,017
CV6	0,448	-0,098	0,1365	-0,030	0,412	0,090	0,353	0,077
T1 twin								
T1V1	0,342	0,060	0,352	0,062	0,013	-0,002	0,002	0,000
T1V2	0,414	0,073	0,377	0,066	0,297	-0,052	0,303	-0,053
T1V3	0,393	0,069	0,305	0,053	0,011	-0,002	0,006	0,001
T1V4	0,381	0,067	0,225	0,039	0,430	-0,075	0,390	-0,068
T1V5	0,422	0,074	0,351	0,061	0,290	-0,051	0,281	-0,049
T1V6	0,323	0,057	0,298	0,052	0,439	-0,077	0,415	-0,073

Table 5: secondary twin: Calculation of SF and ε'_{33} for different orientations and twin families

	Primary twin : tension twin				**Primary twin : compression twin**			
	Orientation of grain:{64.4, 161.1, 11.7}		Orientation of grain:{162.4, 20.9, 38.9}		Orientation of grain:{108.5, 83.5, 49.3}		Orientation of grain:{16.5, 90.3, 51.7}	
C twin	SF	ε'_{33}	SF	ε'_{33}	SF	ε'_{33}	SF	ε'_{33}
CV1	0,295	-0,064	**0,478**	-0,104	0,376	0,082	**0,444**	0,097
CV2	0,357	-0,078	0,370	-0,081	0,059	0,013	0,061	0,013
CV3	0,471	-0,103	0,209	-0,046	**0,472**	0,103	0,439	0,096
CV4	**0,488**	-0,106	0,247	-0,054	0,215	0,047	0,172	0,038
CV5	0,441	-0,096	0,414	-0,090	0,027	0,006	0,063	0,014
CV6	0,229	-0,050	0,471	-0,103	0,152	0,033	0,175	0,038
T1 twin								
T1V1	0,449	0,079	0,392	0,069	0,284	-0,050	0,306	-0,054
T1V2	0,437	0,076	0,416	0,073	0,012	-0,002	0,010	-0,002
T1V3	0,438	0,077	0,428	0,075	0,269	-0,047	0,307	-0,054
T1V4	0,374	0,065	0,401	0,070	0,422	-0,074	0,430	-0,0754
T1V5	0,397	0,070	0,437	0,077	0,009	-0,002	0,010	-0,002
T1V6	0,424	0,074	0,344	0,060	0,441	-0,077	0,430	-0,075

In these two tables (4 and 5), the types of twins which is chosen to accommodate the deformation is always the ones which have negative value of ε'_{33}.

To illustrate the possible orientation localization of grains that can generate positive or negative ε'_{33} through compression twinning or tension twinning, 20000 grains with random orientations are artificially generated and represented in their 0002 pole figures, as shown in Fig. 4 a and b, where the positive values of ε'_{33} are in dark gray and the negative values are in gray-white.

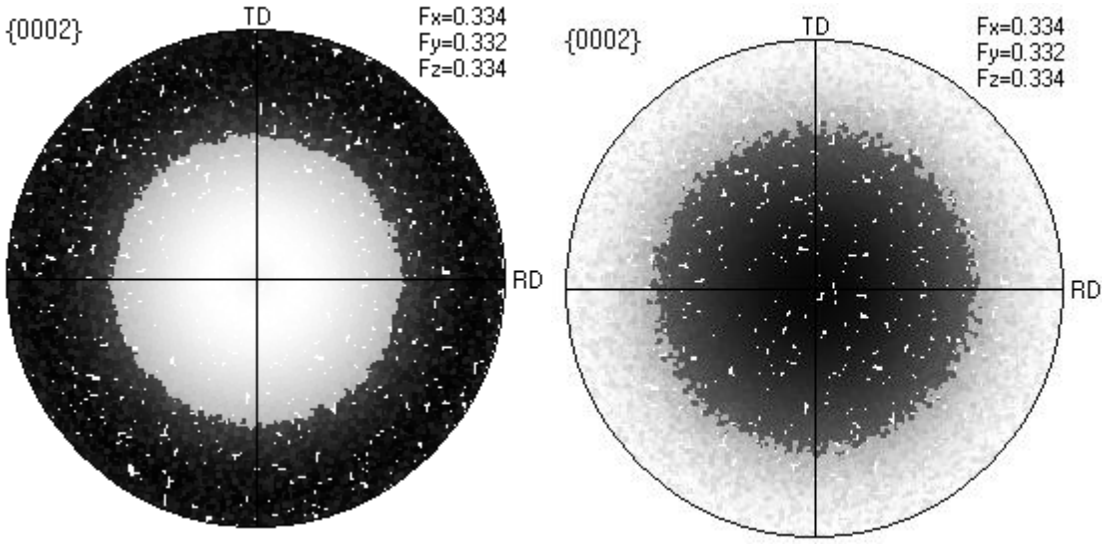

Fig 4:a) (0002) pole figure , where orientations producing positive ε'_{33} during compression twinning (C twin) are in dark gray and those producing negative ε'_{33} are in gray-white. The load is applied in the normal direction.

b) (0002) pole figure , where orientations producing positive ε'_{33} during tension twinning (T1 twin) are in dark gray and those producing negative ε'_{33} are in gray-white. The load is applied in the normal direction.

With this representation, it is easy to know, for a grain orientation, which type of twin may appear in the grain (it is necessary to know the stress state in the third direction).

It is possible to extend the calculation to another type of deformation mode and draw the same pole figure for ε_{11} and ε_{22} (Fig 5). In Fig 5 a and b, grains that can generate positive value of the respective ε'_{11} and ε'_{22} for the load applied in direction 1 (horizontal axis =RD) is in the dark gray zone, whereas those generate negative value is in the gray-white zone. Fig. 5 c and d display when the load is applied in direction 2 (vertical axis =TD).

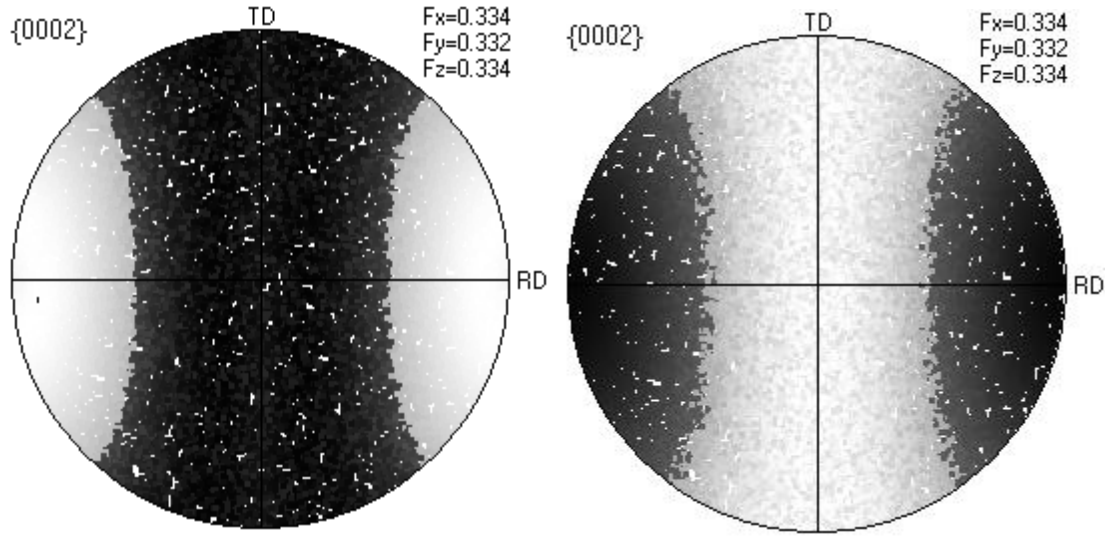

Fig 5: Poles figures

a) (0002) poles figure , where orientations producing positive ε'_{11} during compression twinning (C twinning) is in dark gray and those producing negative ε'_{11} are in gray-white. Load is applied in RD.

b) (0002) poles figure, where orientations producing positive ε'_{11} during tension twinning (C twinning) is in dark gray and those producing negative ε'_{11} are in gray-white. Load is applied in RD.

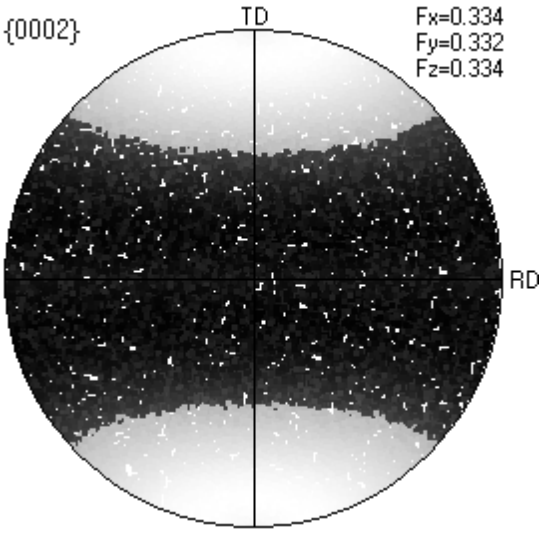

c) (0002) poles figure, where orientations producing positive ε'_{11} during compression twinning (C twinning) is in dark gray and those producing negative ε'_{11} are in gray-white. Load is applied in RD. of ε'_{22} obtain with C twin

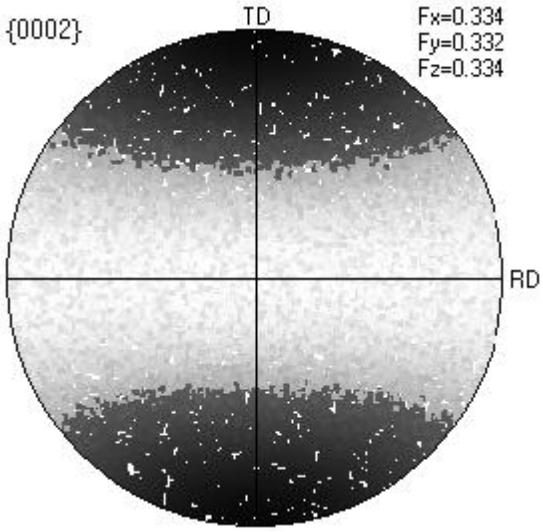

d) (0002) poles figure , where orientations producing positive ε'_{22} during tension twinning (T1 twinning) is in dark gray and those producing negative ε'_{22} are in gray-white. Load is applied in TD.

Discussion

Table 4 and 5 show that the twinning system which is chosen by the material to accommodate the deformation always produces negative ε'_{33}.

The SF is not a sufficient criterion to estimate which type of twin can appears in the grain. In most cases, the twin families with high SF is not chosen in the material.

The energy to propagate a twin ($W_{twin} = \tau\gamma$) is always positive. To satisfy this condition, in equation 11, the deformation must be always negative (in the case of channel die test). The condition could be used to estimate the activation of the twin variants.

The above results demonstrate that the selection of the type of twin is a function of the plastic deformation energy.

To ensure positive energy, compression twins in the grains with their c-axis in the gray-white zone in the above figures can be activated if the local stress is in compression and tension twins in those with their c-axis in the black zone are activated if the local stress state is in tension. The choice of the twin type is determined by the orientation of the grain and by the local stress which depend on the macroscopic stress.

Tables 4 and 5 also show that after tension (or compression) twinning, the twinned area cannot produce a secondary tension (or compression) twin because the deformations in these cases are positive. In fact, twinning changes the position of the c-axis (Fig 6) of the twinned part, thereby transferring the c-axis (84.78 ° for a T1 twin, 74.62 for a C twin) to an area in the pole figure where the strains are positive. Only an opposite twin (C twin if the primary twin was T1 or vice versa) may be activated.

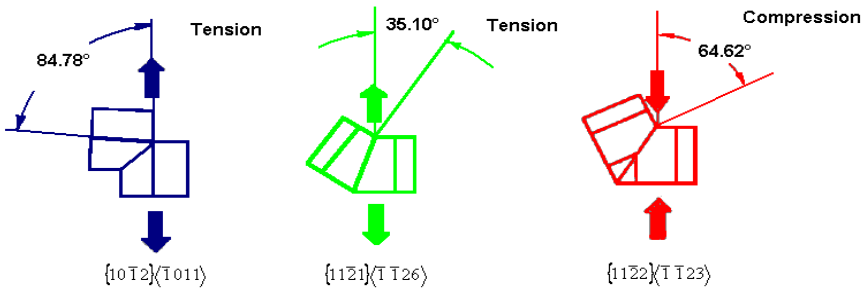

Fig 6: Schematic representation of the rotation of c axis versus type of twin

One may wonder why T2 twins (s= 0.62) are rarely seen in titanium. The ε'_{33} produced during the formation of the twins along the c-axis is as follows. The strains of C twin range from -0.11 to 0.11, the T1 twins range -0.09 to 0.09, whereas strains of tension T2 twin vary between -0.31 to 0.31. Fig. 7 shows the (0002) poles figure, where orientations producing positive ε'_{33} during T2 twinning is in dark gray and those producing negative ε'_{33} are in gray-white, when the external force is applied in the normal direction (ND). Comparing Fig. 7 with Fig. 4 b, one can see that the orientation of grains producing T2 twin with negative strain is overlap with those producing T1 twin with negative strain. In fact, there is a slight overlap between the areas where it is possible to have twins C and to have twins T1. Therefore, according to a given stress state, it will always be easier to activate the T1 or C twins than T2 twins (minimum expenditure of energy). This is why that at the strain level in our work we could not find T2 twins.

However, depending on the orientation of the c-axis of the grain and the local stress state, it is possible to activate this type of twin. The choice is always made under the same energy criteria: ie $W_{twin}>0$ and minimum of microscopical energy

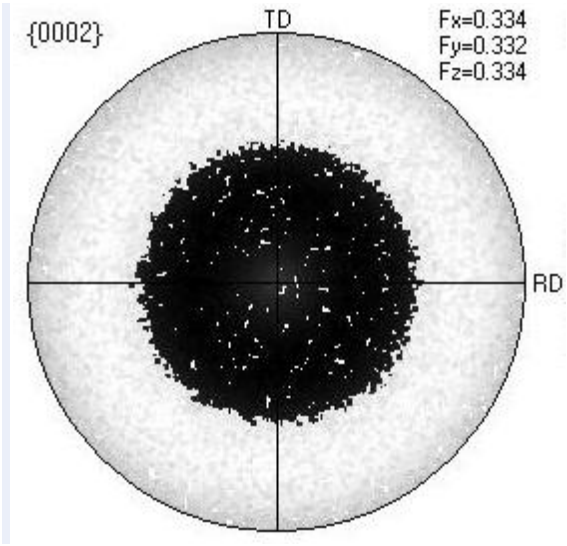

Fig 7 : (0002) poles figure , where orientations producing positive ε'_{11} during T2 twinning is in dark gray and those producing negative ε'_{11} are in gray-white. Load is applied in ND.

For a clear presentation of the choice of possible twin variants under various loading conditions by our proposed criterion, the orientation zone of grains that may produce certain type of twin under compression in RD, TD and ND directions are displayed in the 0002 pole figures in Fig. 8. From these figures, it is easy to find that under certain applied load, which kind of twins could be activated. It is also possible to have in a domain different twins family. The reality is probably a combination of these figures, because the process of plastic shaping can't be reduce to a simple component of the strain tensor.

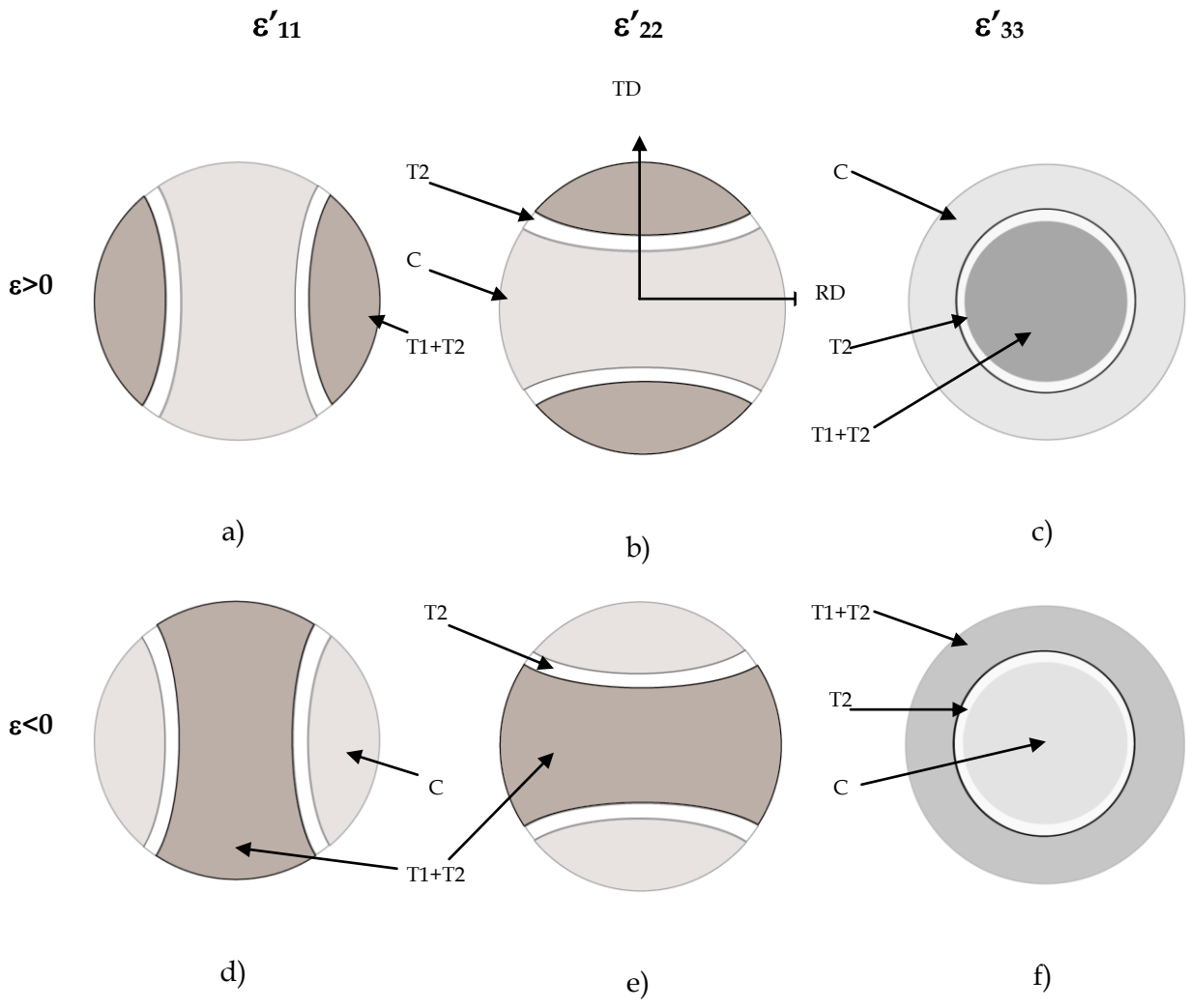

Fig 8: schematic representations of the (0002) pole figures with highlighted orientation areas where it is possible to activate certain twinning system under given deformation loads (gray = C system, white = T2 system, dark gray =T1+T2 system). Our calculated results are not

contradictory with the experimental results (Fig. 9) previously obtained by Le Cras [24]. Fig. 9 was obtained under rolling condition, which is comparable with Fig. 8 f.

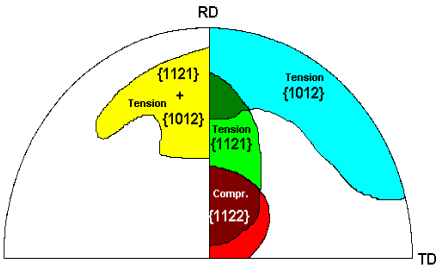

Fig 9: (0002) Poles Figure showing the orientation domains of the <c> axes of the grains in which the indicated twinning is activated [22, 24]

The slight differences between the experimental work and the calculated one may be due to the facts as follow:

-we made calculation in simple case and the rolling cannot be reduce to one component of the strain tensor,

- we did not take into account of the local stress tensor in the grain,

- we did not take into account of the stable orientations (as are shown in Fig 10 a and b). In these orientations we do not have twinning.

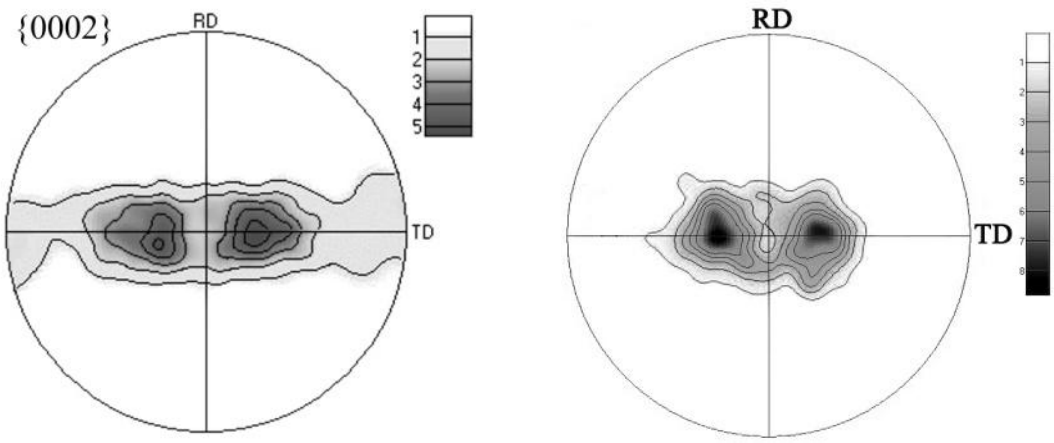

a) annealed b) rolling

Fig 10: (0002) Pole figure of titanium.

In a previous study [28] we have shown that the choice of the type of twin variant is made by the maximization of the absolute value of the ratio $\frac{\varepsilon'_{33}}{\sqrt{L}}$ (where L is the maximum length that a variant can have in the grain).

Conclusion

With the experimental examination, an energetic twin system and twin variant selection rule[28] in titanium during deformation has been proposed. The prediction is correct in 85% () of the cases of primary twinning and correct in 95% of the case of secondary twinning, whereas that according to SF only in less 50%.

The rule is:

1) The choice of the twin system is made by the condition W>0.
2) If several twins family are possible (tension twins : T1 and T2), the system chose the family with less work. In general T1.

3) For a fixed type of twin,, the variant selection is made by , in our case, the absolute value of the ratio $\frac{\varepsilon'_{33}}{\sqrt{L}}$ is maximal.

The choice of a slip or twinning system is based on an energy criterion. The variant selected will be the one that consumes as much as possible the internal energy of the material.

Calculations by ab-initio and EAM (embedded atom method) are undertaken to determine twinning energies. These calculations already led to results in the case of crystallographic slip[25].

Taking account of the value of strain to explain the type of twin and of the grain size [28] seems to be one of the essential factors to explain the variant selection. More precisely, it will introduce the concepts of domain, free path and that of new grain. Thus, a twin will be regarded as a – new - grain characterized by its size and crystallographic orientation. Accordingly, the concept of secondary twinning could be reconsidered.

Acknowledgements:

This work was supported by the Federation of Research for Aeronautic and Space (Fédération de Recherche pour l'Aéronautique et l'Espace Thème Matériaux pour l'Aéronautique et l'Espace : project OPTIMIST (optimisation de la mise en forme d'alliage de titane)).

We are gratefull to Prof Paul Van Houtte for his discussion and comments about this work

References:

[1] Kocks, U.F. and D.G. Westlake, AIME MET SOC TRANS, 1967. **239**(7): p. 1107-1109.

[2] Yoo, M., Metallurgical and Materials Transactions A, 1981. **12**(3): p. 409-418.

[3] M. J. Philippe, M. Serghat, P. Van Houtte, C. Esling. Acta Metall. et Mater. 1995, 43, 1619.

[4] Y. B. Chun, S.H. Yu, S.L. Seliatin, S.K. Hwang, Mater. Sci. Eng. A 2005, 398, 209.

[5] D. H. Shin, I. Kim, J. Kim, Y.T Zhu, Mater. Sci. Eng. A 2002, 334, 239.

[6] L. Bao, J.S. Lecomte, C. Schuman, M.J. Philippe, X. Zhao, C. Esling Adv. Eng. Mater. 2010, 12, 1053.

[7] Crocker, A.G.,. Journal of Nuclear Materials, 1965. **16**(3): p. 306-326.

[8] Mahajan, S. and D.F. Williams, International Metallurgical Reviews, 1973. **18**: p. 43-61.

[9] Akhtar, A., Metallurgical and Materials Transactions A, 1975. **6**(4): p. 1105-1113.

[10] Ishiyama, S., S. Hanada, and O. Izumi, Journal of the Japan Institute of Metals, 1990. **54**(9): p. 976-984.

[11] Churchman, A.T., J. Inst. Metals, 1954. **83**: p. 39-40.

[12] Song, S.G. and G.T. Gray, Acta Metallurgica et Materialia, 1995. **43**(6): p. 2339-2350.

[13] Goo, E. and K.T. Park, Scripta metallurgica, 1989. **23**(7): p. 1053-1056.

[14] Proust, G., C.N. Tomé, and G.C. Kaschner, Acta Materialia, 2007. **55**(6): p. 2137-2148.

[15] X. Wu, K. Kalidindi, S.R. Necker, C. Salem, Acta Mater. 2007, 55, 423.

[16] Wonsiewicz, B.C. and W.A. Backofen, Transactions of The Metallurgical Society of AIME, 1967. **239**.

[17] Partridge, P.G., Metallurgical Reviews, 1967. **12**(118): p. 169-194.

[18] Meyers, M.A., O. Vöhringer, and V.A. Lubarda, Acta Materialia, 2001. **49**(19): p. 4025-4039.

[19] Philippe, M.J., C. Esling, and B. Hocheid, Textures and Microstructures, 1988. **7**: p. 265-301.

[20] F. Le Cras, M. serghat, J.J. Fundenberger, M.J. Philippe, C. Esling Proc. Titanium 95, 1, 659.

[21] J. J. Fundenberger, , M.J. Philippe, F. Wagner, C. Esling. Acta Mater. 1997, 45, 4041. &

[22] T.A. Mason, J.F. Bingert, G.C. Karschner, S.I. Wright, R.J. Larsen, Metall. Mater. Trans. A 2002, 33, 949.

[23] L. Bao, C. Schuman, J.S. Lecomte, M.J. Philippe, X. Zhao, L. Zuo, C. Esling. Comput, Mater, Con. 2010, 15, 113.

[24] E. Martin, L. Capolongo, L. Jiang, J.J. Jonas, Acta Mater. 2010, 58, 3970.

[25] J. J. Jonas, S. Mu, T. Al-Samman, G. Gottstein, L. Jiang, E. Martin Acta Mater. 2011, 59, 2046.

[26] A. Poty,J.M. Raulot, H.Xu, D. Rodney, J. Bai, C. Schuman, J.S. Lecomte, M.J. Philippe, C. Esling. J. Appl. Phys, vol 110 Issue 1 , 2011

[27] J. J. Jonas, S. Mu, T. Al-Samman, G. Gottstein, L. Jiang, E. Martin Acta Materialia, Volume 59, Issue 5, March 2011, p 2046

[28] C. Schuman, L. Bao, J.S. Lecomte, Y. Zhang, J.M. Raulot, M.J. Philippe, C. Esling, Adv. Eng. Mat., (2011)

[29] R.E. Reed-Hill, J.P. Rosi, H.C. Rogers, Deformation twinning, vol 25, (1964), Gordon and Breach science publishers

[30] E. Tenckhoff, Deformation mechanism texture and anisotropy in zirconium and zircaloy, ASTM , special technical publication STP 966, 1988)